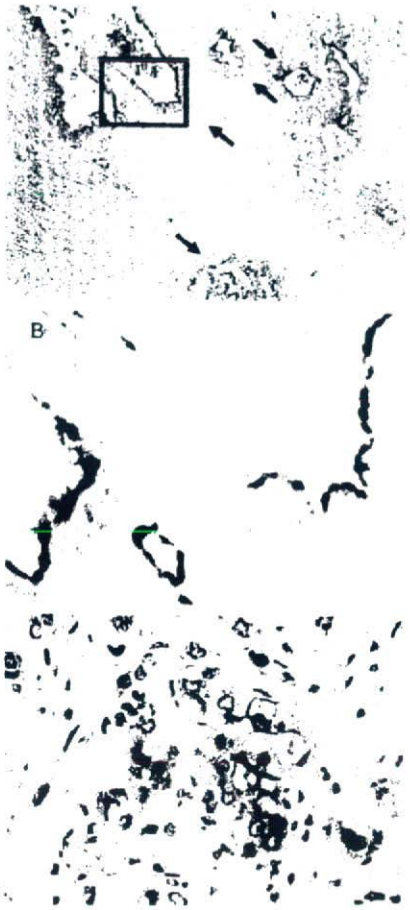

Figure 2. C-ERC/mesothelin expression in human pancreatic cancer tissue. (A) Immunohistochemical staining of C-ERC/mesothelin using 5B2 antibody, magnification (x40). Positive staining is shown by arrows. (B) Same sample as (A), respectively, with higher magnification (x200). An area covered by a square frame in (A) is expanded. (C) Another 5B2 stained sample with magnification (x200).

Table I. C-ERC/mesothelin immunostaining results of human pancreatic ductal carcinoma.

	Intensity			Proportion			
Sample	1+	2+	3+	0	<10	10-50	>50
FNA	3	1	2	5	3	1	2
Operation	2	4	2	0	1	4	3
Total	5	5	4	5	4	5	5

The intensity of staining was semiquantitatively graded on a scale of 1+ to 3+ and the proportion of stained ducts of cancer gland was graded as 0%, 1 to <10%, 10-50%, >50%.

concentration between cancer patients and the healthy control group (P=0.569) (Fig. 3A). Between patients with resectable tumor and those with far advanced unresectable tumor, there was no significant difference in serum N-ERC/mesothelin concentration (P=0.710) (Fig. 3B).

Discussion

In the present study, we examined C- and N-ERC/mesothelin expression in the two patients with pancreatic ductal carcinoma and cultured pancreatic cancer cell lines. The expression of C-ERC/mesothelin was studied by immunoblotting of cultured cell lysates or by immunohistochemical staining of carcinoma tissue. The concentration of N-ERC/mesothelin in the supernatant of cultured cells or in sera of patients was measured by the ELISA system established by us (5-7). Our study indicated that N-ERC/mesothelin concentration in supernatants correlated with the expression levels of C-ERC/mesothelin in cultured cells. Human pancreatic ductal carcinoma frequently expressed C-ERC/mesothelin. Contrary to our initial expectation, we did not find any significant difference in the

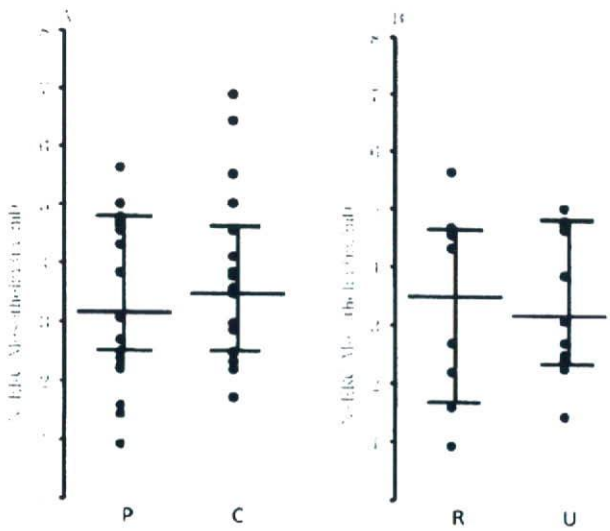

Figure 3. Scatter plots of serum N-ERC/mesothelin concentration. (A) Comparison of N-ERC/mesothelin concentration in sera from patients with pancreatic ductal carcinoma (P) and healthy controls (C). (B) Comparison of patients with resectable tumor (R) and unresectable far advanced tumor (U).

serum concen-tration of N-ERC/mesothelin between patients with pancreatic ductal carcinoma and normal controls.

Almost all human pancreatic cancer cell lines, except for MIA-PaCa2, expressed mRNA of ERC/mesothelin. KP-3 and TCC-PAN2 strongly expressed C-ERC/mesothelin protein and secreted high amounts of N-ERC/mesothelin, while MIA-PaCa2 did not express C-ERC/mesothelin nor secrete N-ERC/mesothelin at all. N-ERC/mesothelin concentration in the supernatants of cultured cells almost correlated with C-ERC/mesothelin expression.

All surgically resected samples showed positive staining for C-ERC/mesothelin. However, five of 11 FNA cases showed negative staining. Baruch *et al* reported that >50% of samples from FNA are negative for C-ERC/mesothelin because the staining pattern is most often focal and unevenly distributed (16). Argani *et al* reported that in tissue sections of pancreatic adenocarcinomas, diffuse staining was seen in only 30% of the mesothelin positive tumors (15). There is the possibility that our staining data of FNA samples, as shown in Table I, may have underestimated the actual expression of C-ERC/mesothelin because of the small and limited volume of FNA samples. Either way, we and others have shown that human pancreatic ductal carcinoma frequently expressed C-ERC/mesothelin. The staining pattern of pancreatic ductal carcinoma was cytoplasmic with or without polarity to apical membrane, while that of mesothelioma was membranous (1,5,7,17,20).

Based on these results, we investigated whether the serum level of N-ERC/mesothelin could be a novel diagnostic marker of human pancreatic ductal carcinoma, using our previously reported ELISA system for detection (5-7). We age-matched the patients and healthy controls, because N-ERC/mesothelin in the sera has a tendency to elevate as people get older. Unexpectedly, we found that N-ERC/mesothelin in sera of patients with pancreatic ductal carcinoma was comparable to those of healthy controls.

Other ERC/mesothelin expressing tumors, including ovarian cancers and mesotheliomas, can be detected by measurement of serum C- or N-ERC/mesothelin concentration (5-12). We have shown that our ELISA system for N-ERC/mesothelin also detects mesotheliomas (5-7). Presently, the reason why N-ERC/mesothelin was not increased in the sera of patients with pancreatic ductal carcinoma while C-ERC/mesothelin was frequently expressed in the carcinoma tissues is unknown. In the far advanced pancreatic ductal carcinoma patients with stage IV disease, N-ERC/mesothelin concentration was not higher than in the patients with stage I-III diseases (data not shown). Thus, it appears that the proportion of C-ERC/mesothelin expressing ducts of the gland was not the reason. It was considered that differences between *in vitro* and *in vivo* conditions, for example changes in the micro-environments such as differential expression of proteases and their inhibitors, or tumor vascularity, may contribute to this discrepancy. High concentration of serum N-ERC/mesothelin indicates a patient that does not have pancreatic ductal carcinoma, but other C-ERC/mesothelin expressing tumor, perhaps mesothelioma. In this case, examination for pancreatic ductal carcinoma could be omitted.

In conclusion, N-ERC/mesothelin concentration in supernatants correlated with the expression levels of C-ERC/mesothelin in cultured cells. Human pancreatic ductal carcinoma frequently expressed C-ERC/mesothelin. However, serum N-ERC/mesothelin concentration of cancer patients was equivalent to healthy controls. N-ERC/mesothelin was not useful as a serum marker of pancreatic ductal carcinoma. Because of frequent expression of C-ERC/mesothelin in pancreatic ductal carcinoma tissues, there is a possibility that imaging detection system or immunotherapy, using C-ERC/mesothelin, will be developed in the future.

Acknowledgments

We would like to thank, Masumi Maruo, Naoko Aoki, Kazu Shiomi, Danqing Zhang, Toshiyuki Kobayashi and members of the Department of Gastroenterology, Juntendo hospital, for their help in management of this study. This work is supported by a Grant-in-Aid for Cancer Research and Grants-in-Aid for Scientific Research from the Ministry of Education, Culture, Sports and Science and Technology of Japan and the Ministry of Health, Labor and Welfare of Japan. This study was partially supported by a consignment expense for Molecular Imaging Program on 'Research Base for PET Diagnosis' from Ministry of Education, Culture, Sport and Science and Technology, Government of Japan.

References

1. Chang K and Pastan I: Molecular cloning of mesothelin, a differentiation antigen present on mesothelium, mesotheliomas, and ovarian cancers. Proc Natl Acad Sci USA 93: 136-140, 1996.
2. Hassan R, Bera T and Pastan I: Mesothelin: a new target for immunotherapy. Clin Cancer Res 10: 3937-3942, 2004.
3. Yamaguchi N, Hattori K, Oh-eda M, Kojima T, Imai N and Ochi N: A novel cytokine exhibiting megakaryocyte potentiating activity from a human pancreatic tumor cell line HPC-Y5. J Biol Chem 269: 805-808, 1994.
4. Kojima T, Oh-eda M, Hattori K, *et al*: Molecular cloning and expression of megakaryocyte potentiating factor cDNA. J Biol Chem 270: 21984-21990, 1995.
5. Shiomi K, Miyamoto H, Segawa T, *et al*: Novel ELISA system for detection of N-ERC/mesothelin in the sera of mesothelioma patients. Cancer Sci 97: 928-932, 2006.
6. Shiomi K, Hagiwara Y, Sonoue K, *et al*: Sensitive and specific new enzyme-linked immunosorbent assay for N-ERC/Mesothelin increases its potential as a useful serum tumor marker for mesothelioma. Clin Cancer Res 14: 1431-1437, 2008.
7. Hino O and Shiomi K: Diagnostic biomarker of asbestos-related mesothelioma: Example of translational research. Cancer Sci 98: 1147-1157, 2007.
8. Scholler N, Fu N, Yang Y, *et al*: Soluble member(s) of the mesothelin/megakaryocyte potentiating factor family are detectable in sera from patients with ovarian carcinoma. Proc Natl Acad Sci USA 96: 11531-11536, 1999.
9. Onda M, Nagata S, Ho M, *et al*: Megakaryocyte potentiation factor cleaved from mesothelin precursor is a useful tumor marker in the serum of patients with mesothelioma. Clin Cancer Res 12: 4225-4231, 2006.
10. Hassan R, Remaley AT, Sampson ML, *et al*: Detection and quantitation of serum mesothelin, a tumor marker for patients with mesothelioma and ovarian cancer. Clin Cancer Res 12: 447-453, 2006.
11. Robinson BW, Creaney J, Lake R, *et al*: Mesothelin-family proteins and diagnosis of mesothelioma. Lancet 15: 1612-1616, 2003.
12. Robinson BW, Creaney J, Lake R, Nowak A, Musk AW, de Klerk N, Winzell P, Hellstrom KE and Hellstrom I: Soluble mesothelin-related protein - a blood test for mesothelioma. Lung Cancer 49: S109-S111, 2005.

13. Sapede C, Gauvrit A, Barbieux I, *et al*: Aberrant splicing and protease involvement in mesothelin release from epithelioid mesothelioma cells. Cancer Sci 99: 590-594, 2008.
14. Chang K, Pastan I and Willingham M: Frequent expression of the tumor antigen CAK1 in squamous-cell carcinomas. Int J Cancer 51: 548-554, 1992.
15. Argani P, Iacobuzio-Donahue C, Ryu B, *et al*: Mesothelin is overexpressed in the vast majority of ductal adenocarinomas of the pancreas: identification of a new pancreatic cancer marker by serial analysis of gene expression (SAGE). Clin Cancer Res 7: 3862-3868, 2001.
16. Baruch AC, Wang H, Staerkel GA, Evans DB, Hwang RF and Krishnamurthy S: Immunocytochemical study of the expression of mesothelin in fine-needle aspiration biopsy specimens of pancreatic adenocarcinoma. Diagn Cytopathol 35: 143-147, 2007.
17. Yaziji H, Battifora H, Barry TS, *et al*: Evaluation of 12 antibodies for distinguishing epithelioid mesothelioma from adenocarcinoma: identification of a three-antibody immunohistochemical panel with maximal sensitivity and specificity. Mod Pathol 19: 514-523, 2006.
18. Segawa T, Hagiwara Y, Ishikawa K, *et al*: MESOMARK kit detects C-ERC/mesothelin, but not SMRP with C-terminus. Biochem Biophys Res Commun 369: 915-918, 2008.
19. Yamashita Y, Yokoyama M, Kobayashi E, Takai S and Hino O: Mapping and determination of the cDNA sequence of the Erc gene preferentially expressed in renal cell carcinoma in the Tsc2 gene mutant (Eker) rat model. Biochem Biophys Res Commun 275: 134-140, 2000.
20. Maeda M and O Hino: Molecular tumor marker for asbestos-related mesothelioma: serum diagnostic markers. Pathol Int 56: 649-654, 2006.
21. Maeda M and O Hino: Blood test for asbestos-related mesothelioma. Oncology 71: 26-31, 2006.
22. Wray CJ, Ahmad SA, Matthews JB and Lowy AM: Surgery for pancreatic cancer: recent controversies and current practice. Gastroenterology 128: 1626-1641, 2005.
23. Li D, Xie K, Wolff R and Abbruzzese JL: Pancreatic cancer. Lancet 363: 1049-1057, 2004.
24. Matsuno S, Egawa S, Fukuyama S, *et al*: Pancreatic cancer registry in Japan: 20 years of experience. Pancreas 28: 219-230, 2004.
25. Egawa S, Takeda K, Fukuyama S, Motoi F, Sunamura M and Matsuno S: Clinicopathological aspects of small cancer. Pancreas 28: 235-240, 2004.
26. Chomczynski P and Sacchi N: Single-step method of RNA isolation by acid guanidinium thiocyanate-phenol-chloroform extraction. Anal Biochem 162: 156-159, 1987.

Establishment of a novel specific ELISA system for rat N- and C-ERC/mesothelin. Rat ERC/mesothelin in the body fluids of mice bearing mesothelioma

Yoshiaki Hagiwara,[1,2] Yukiko Hamada,[1] Maki Kuwahara,[3] Masahiro Maeda,[1] Tatsuya Segawa,[1] Kiyoshi Ishikawa[1] and Okio Hino[2,4]

[1]Immuno-Biological Laboratories, 5-1 Aramachi, Takasaki-Shi, Gunma 370-0831; [2]Department of Pathology and Oncology, Juntendo University, School of Medicine, 2-1-1 Hongo, Bunkyo-Ku, Tokyo 113-8421; [3]Laboratory of Pathology, Toxicology Division, The Institute of Environmental Toxicology, 4321 Uchimoriyamachi, Jousou, Ibaraki, 303-0043, Japan

(Received September 21, 2007/Revised November 8, 2007/2nd Revision Novembr 21, 2007/Accepted December 2, 2007)

Mesothelioma is a type of malignant tumor that most commonly arises from the pleural or peritoneal membrane and is usually associated with previous exposure to asbestos. In humans, ERC/mesothelin is expressed on the normal mesothelium and in some cancers such as mesothelioma or ovarian carcinoma. Recently, several enzyme-linked immunosorbent assay (ELISA) systems for ERC/mesothelin have been developed, the reported usefulness of which has been assessed and demonstrated as a diagnostic tool. However, the basic roles or physiological functions of, and relationship between, ERC/mesothelin and asbestos exposure-mediated carcinogenesis remain to be resolved. In order to elucidate the precise mechanism, animal models of mesothelioma are desperately needed. In this study, we consider the development of a novel specific ELISA system for not only rat N-ERC/mesothelin but also C-ERC/mesothelin, and the first data on the presence of rat ERC/mesothelin in the body fluids of rat malignant mesothelioma-bearing nude mice. The transplanted mice have revealed the higher concentrations of rat N-ERC/mesothelin in the blood and ascites than C-ERC/mesothelin. We hope these novel ELISA systems are useful in the rat model system to clarify the mechanism of asbestos-induced carcinogenesis and to develop new effective drugs for mesothelioma. (*Cancer Sci* 2008)

The number of cases of mesothelioma caused by exposure to asbestos is growing, and as exemplified by the shocking events in 2005 and highlighted in TV and newspaper reports every day in Japan, this condition represents an enormous social problem.

Mesothelioma is a type of malignant tumor that most commonly arises from the pleural or peritoneal membrane. It is believed that mesothelioma is caused by the inhalation of asbestos fibers. However, how the aspirated asbestos in the lung might provoke tumor formation in the pleural membrane that covers the lungs, or the peritoneal membrane, has not yet been clarified.[1,2]

In regard to human mesothelioma, a group from Australia has reported that soluble mesothelin-related protein (SMRP), the C-terminal fragment of mesothelin, may be a tumor marker. Another group from National Institute of Health has reported that the N-terminal fragment of mesothelin may be a mesothelioma marker.[3–11] Also, Shiomi *et al.* reported the usefulness of the N-ERC/mesothelin as a serum marker for mesothelioma.[9]

The mesothelin protein is present in the normal mesothelium, a membrane lining several body cavities including the pleura, peritoneum, and pericardium. It could be speculated that mesothelioma derived from the mesothelium should demonstrate overexpression of mesothelin. This protein, 622 amino acids in length, is expressed as a GPI anchor-type membranous protein of with a molecular weight of about 71 kDa, that is cleaved by a furin-like protease into the 31 kDa N-terminal fragment and 40 kDa C-terminal fragment.

On the other hand, we have conducted research on the Eker model rat, a rat model of renal cell calcinoma, and cloned the *Erc* gene, which is expressed in abundance in the kidney of Eker rats. The expected amino acid sequence of the rat *Erc* cDNA exhibits 87.4% similarity to the mouse protein and 56.1% similarity to human MPF/mesothelin. Although the similarity to the human protein is not so high, both the sequences possess two hydrophobic regions, secretory signal sequences at the N terminus, signal sequences characteristic of a GPI anchor-type protein at the C terminal, secretory recognition sequences for a furin-like protease, and are located in the same chromosome as the tumor suppresser *Tsc2/TSC* gene. Based on the above, it is considered that the rat ERC may be a functional orthologue of human mesothelin; therefore, we call this gene product ERC/mesothelin.

We attempted to develop a rat ERC/mesothelin ELISA assay kit following the idea that ERC/mesothelin may be a potentially useful marker of malignant mesothelioma in humans, since the possible existence of a strong relationship between ERC/mesothelin and mesothelioma in humans has been suggested.

Shiomi *et al.* have developed a human ERC/mesothelin ELISA assay kit and reported that ERC/mesothelin is a useful marker for malignant mesothelioma.[9]

Nakaishi *et al.* established an assay system using mouse monoclonal antibody (MoAb) 30F2 as the solid antibody and a polyclonal antibody of N-ERC (150–160) as the enzyme-labeled antibody, for detecting the N-terminal fragment, N-ERC, of ERC/mesothelin. They measured the blood concentrations of N-ERC/mesothelin in the Eker rat, a model of renal cell carcinoma using this assay system.[12]

In this study, to investigate whether ERC/mesothelin could be a mesothelioma marker in the rat and to investigate the functions of ERC/mesothelin in relation to the development and progression of mesothelioma, we developed a novel highly specific and sensitive sandwich ELISA system for not only rat N-ERC/mesothelin but also C-ERC/mesothelin. Moreover, a Xenograft mouse model for mesothelioma has been developed.

Using these novel ELISA systems, we determined the presence of ERC/mesothelin in the body fluids of tumor-bearing nude mice, in order to explore the potential usefulness of this protein as a marker of mesothelioma.

Materials and Methods

Production of antibodies. ***Production of rabbit PoAb.*** We synthesized synthetic peptides corresponding to the peptide sequences 150–166, 259–280, 306–327, and 549–566 of full-length rat ERC/

[4]To whom correspondence should be addressed. E-mail: ohino@med.juntendo.ac.jp

doi: 10.1111/j.1349-7006.2008.00731.x

mesothelin and immunized rabbits. Each antiserum was purified by affinity column chromatography using an antigen peptide-coupled solid-phase column.

Production of mouse MoAb. MoAb 30F2[12] was purified from the resultant ascitic fluid of transplanted mice with hybridoma cells with a protein A column.

Western blotting. The full-length rat ERC/mesothelin cDNA was transfected into CHO-K1 cells and the cell culture supernatant was collected. The supernatant was subjected to Western blot analysis with N-ERC (150–166) and N-ERC (259–280) PoAb, and rat C-ERC (549–566) and rat C-ERC (306–327) PoAb. Secondary antibodies in the form of goat antirabbit IgG conjugated to peroxidase (No. 17502; Immuno-Biological Laboratories Co. Ltd. (IBL), Gumna, Japan) were then added and allowed to react with the membranes at room temperature for 1 h. ERC/mesothelin on the membranes was visualized by the ECL detection system (Amersham Biosciences, GE Healthcare UK Ltd., Buckinghamshire, England).

Epitope Mapping of MoAb. We produced four different molecular sizes of the GST-fusion protein by cutting the rat ERC/mesothelin gene into four 0.2 kb fragments.

The samples were electrophoresed on 12.5% Laemmli gel, and transferred to a polyvinylidene difluoride memblane.

The membrane was incubated with 1 μg/mL of the first group of antibodies (30F2 MoAb; N-ERC [259–280] PoAb) in phosphate-buffered saline (PBS) for 1 h, incubated with the second group of antibodies, and then detected as described in the section above.

Establishment of the ELISA assay system

Production of standard rat ERC/mesothelin protein for the ELISA system. The full-length cDNA of the rat ERC/mesothelin coding region was inserted into the pcDNA3.1(+) vector (Invitrogen, Carlsbad, CA, USA) and transfected into CHO-K1 cells. The culture supernatant of the stable transfectant was collected and applied on affinity column chromatography using 30F2 MoAb. The eluate was additionally purified with affinity column chromatography using N-ERC (259–280) PoAb. The concentration of purified protein was measured by protein assay (Bio-Rad, Tokyo, Japan). The purity of the protein was demonstrated densitometrically by using a densitograph (ATTO, Tokyo, Japan) and gel-filtration chromatography (data not shown). This affinity-purified rat N-ERC/mesothelin was used as the ELISA standard.

Establishment of the ELISA system. An Immuno Module Plate (Nalge Nunc, Rochester, NY, USA) was coated with the 30F2 MoAb (in 0.1 mol carbonate buffer, pH 9.5) and incubated at 4°C overnight, then blocked with 1% bovine serum albumin in PBS. The sample and standard N-ERC/mesothelin proteins were diluted with 0.05% Tween 20 in PBS and added to each well, followed by incubation of the well at 37°C for 1 h. After nine washes with the washing buffer, 100 μL of horseradish peroxidase-labeled N-ERC (259–280) PoAb was added to each well, followed by incubation for 30 min at 4°C. After nine washes with the washing buffer, 100 μL of tetramethyl benzidine buffer was added as the substrate to each well, followed by incubation for 30 min at room temperature in the dark. Color development was stopped by the addition of 100 μL of stop solution (1 N H_2SO_4). The optical density of each sample at 450 nm was then measured.

The same protocol was employed for the assay of rat C-ERC/mesothelin.

For this assay, the Immuno Module Plate was coated with rat C-ERC (549–566) PoAb, and rat C-ERC (306–327) PoAb was used as a horseradish peroxidase-labeled antibody.

Immunohistochemistry of rat ERC/mesothelin in Wistar rats. Four-micrometer-thick tissue sections were prepared from the formalin-fixed, paraffin-embedded tissue of Wistar rats. After deparaffinization, the tissue sections were heated in 10 mmol citrate buffer (pH 6.0) for antigen retrieval, and treated with 3% hydrogen peroxide. Then, the sections were incubated with 1 μg/mL of a primary rat C-ERC (549–566) PoAb in PBS-T at room temperature overnight. Envision K4002 (Dako Japan Co. Ltd., Kyoto, Japan) was applied to the tissue sections, without dilution, as the secondary antibody. Diaminobenzidine (DAB) was used as the substrate for peroxidase.

FACS analysis. We confirmed the expressions of rat ERC/mesothelin in the cultured cells of the rat mesothelioma cell line (MeET-4)[13] and Yoshida salcoma (YS),[14] using rat C-ERC/mesothelin antibodies.

Cells were cultured in TIL medium (No. 33612; IBL, Gunma, Japan) containing 10% FCS, washed, and susupended to obtain 2×10^6 cells/mL/50 μL/tube.

The cells were incubated with 5 μg/mL of the primary antibody (Rat C-ERC [549–566] and [306–327] PoAb) for 1 h at 4°C.

Goat antirabbit IgG conjugated to fluorescein-isothiocyanate (No. 17522, IBL) was used as the secondary antibody; it was applied at 50 μg/mL or 20 μL to each well, followed by incubation at 4°C for 20 min. FACS analysis was then conducted.

Intraperitoneal transplantation of mesothelioma cells in nude mice and measurement of rat ERC/mesothelin in the body fluids. MeET-4 and YS cells were cultured in TIL medium containing 10% FCS, washed, and suspended with physiological saline solution to obtain 1×10^7/0.5 mL.

The cell suspensions were injected hypodermically into the abdominal cavity of nude mice (Balb/c 6–8 week old females; Charles River Laboratories, Kanagawa, Japan).

The ascitic fluid and serum specimens were collected 8 and 12 days after transplantation and the concentration of N- and C-ERC/mesothelin was measured using the specific ELISA systems.

Results

Specificity of the antibodies. The specificities of the antibodies were confirmed by Western blot analysis of the culture supernatant.

The 30-kDa N-ERC/mesothelin fragment was detected using rat N-ERC (150–166) or N-ERC (259–280) antibodies, and the 40-kDa C-ERC/mesothelin fragment was detected using rat C-ERC (549–566) and rat C-ERC (306–327) antibodies (Fig. 1a).

Epitope mapping of 30F2 MoAb. Antirat ERC/mesothelin (30F2) mouse MoAb reacted with all the GST-fusion proteins prepared with peptide fragments cut from the rat ERC/mesothelin.

We confirmed that the epitope of 30F2 MoAb was on the N-terminal portion of ERC/mesothelin (Fig. 1b).

Establishment of the ELISA system. We used mouse 30F2 MoAb as the solid antibody and the HRP-conjugated rat N-ERC (259–280) rabbit PoAb as the enzyme-labeled antibody in the novel N-ERC/mesothelin assay kit (No. 27765; IBL, Gunma, Japan) (Fig. 2).

For the rat C-ERC/mesothelin assay kit, we used rat C-ERC (549–566) rabbit PoAb as the solid antibody and HRP-conjugated rat C-ERC (306–327) rabbit PoAb as the enzyme-labeled antibody (No. 27761; IBL). The results exhibited a linear log/log plot for the recombinant rat N-ERC/mesothelin concentration range between 0.078 ng/mL and 5.0 ng/mL by N-ERC/mesothelin assay kit, and the recombinant rat C-ERC/mesothelin range between 0.1 ng/mL and 7.0 ng/mL by C-ERC/mesothelin assay kit (Fig. 3).

Determination of the presense of rat ERC/mesothelin in the cell culture supernatant by ELISA system. We determined the presence of rat ERC/mesothelin in the cell culture supernatant using the following method. MeET-4, YS, and rat ERC/mesothelin/CHO cells (5×10^4) were seeded into 24-well culture plates. Culture supernatants were then collected from four wells at various time-points.

The concentration of rat ERC/mesothelin was increased with the increasing proliferative activity of the MeET-4 cells.

doi: 10.1111/j.1349-7006.2008.00731.x

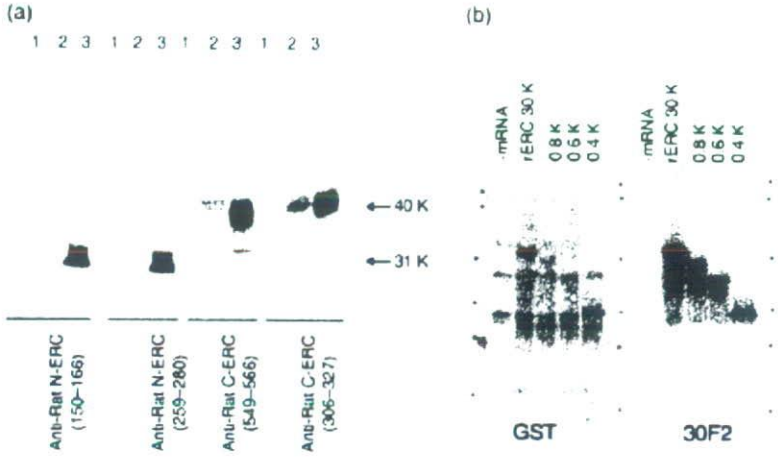

Fig. 1. Characterization of anti-ERC/mesothelin antibodies. (a) Western blot analysis lane 1, MeET-4 cell lysate; lane 2, lysates of MeET-4 subcutaneously transplanted into nude mouse; and lane 3, culture supernatant of rat ERC/CHO transfectant. (b) The Epitope mapping of antirat ERC/mesothelin MoAb (30F2). Four different molecular sizes of the rat ERC/mesothelin fused with GST protein were produced and underwent Western blot analysis by 30F2 MoAb. 30F2MoAb reacted with all the GST-fusion proteins.

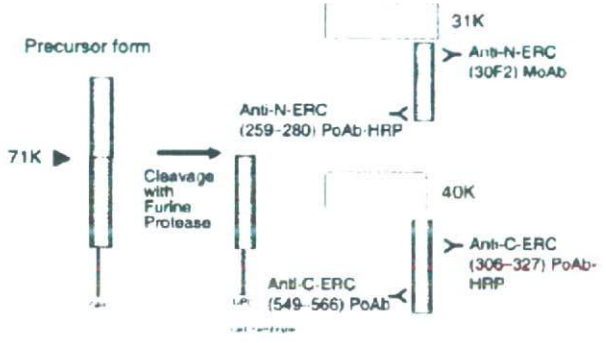

Fig. 2. Products of ERC/mesothelin gene and enzyme-linked immunosorbent assay (ELISA) system. We used mouse 30F2 MoAb as the solid antibody and the HRP-conjugated rat N-ERC (259–280) rabbit PoAb as the enzyme-labeled antibody in the novel N-ERC/mesothelin assay kit. For the Rat C-ERC/mesothelin assay kit, we used rat C-ERC (549–566) rabbit PoAb as the solid antibody and HRP-conjugated rat C-ERC (306–327) rabbit PoAb as the enzyme-labeled antibody.

However, N- and C-ERC/mesothelin were not detected in the YS cells (Fig. 4). These results corresponded with the mRNA expression of ERC/mesothelin by reverse transcription–polymerase chain reaction method (data not shown).

Intraperitoneal transplantation of mesothelioma cells in nude mice and measurement of rat ERC/mesothelin in the body fluids. The concentrations of rat N-ERC and C-ERC/mesothelin in the blood and ascitic fluid of nude mice transplanted intraperitoneally with MeET-4 and YS cells were measured by the specific ELISA systems.

As a result, the ascites with the transplantation of MeET-4 into abdominal cavity showed quite high concentrations of N- and C-ERC/mesothelin (727.5 ng/mL to 2680.5 ng/mL of N-ERC/mesothelin, 108 ng/mL to 251.5 ng/mL of C-ERC/mesothelin). The serum harvested showed a relatively high concentration (511.2 ng/mL to 1075.8 ng/mL of N-ERC/mesothelin, 32.7 ng/mL to 60.8 ng/mL of C-ERC/mesothelin). The serum harvested from mice that underwent subcutaneous transplantation of MeET-4 showed a low concentration of N- and C-ERC/mesothelin (357.6 ng/mL to 605.8 ng/mL of N-ERC/mesothelin, 6.3 ng/mL to 10.4 ng/mL of C-ERC/mesothelin). (Fig. 5). The ERC/mesothelin in mouse body fluids detected by each ELISA system should be of rat MeET-4 origin, because of tjhe absence of detectable amounts of rat ERC/mesothelin concentrations without transplantation.

The N- or C-ERC/mesothelin was not detected in the ascites and serum with the transplantation of YS cells.

In almost all cases when ERC/mesothelin was detected, the concentrations of N-ERC/mesothelin were higher than the concentrations of C-ERC/mesothelin. N-ERC/mesothelin might thus be considered a good marker compared to C-ERC/mesothelin.

Immunohistochemistry. The results of immunohistochemistry confirmed the expression of rat ERC/mesothelin in the lung (Fig. 6a).

FACS analysis. Cell surface expression of the ERC/mesothelin was confirmed using the specific antibody against rat C-ERC/mesothelin, in both MeET-4 and YS1567 cells (Fig. 6b).

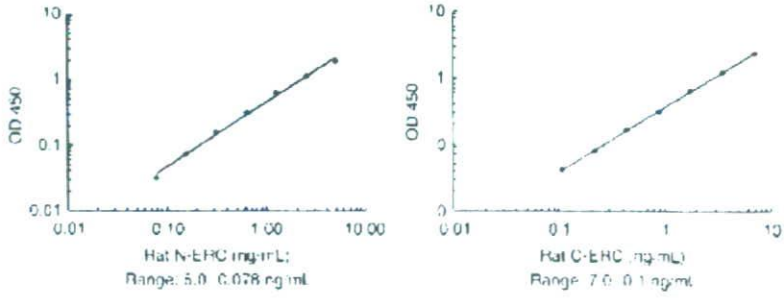

Fig. 3. Typical standard curves of rat ERC/mesothelin enzyme-linked immunosorbent assay (ELISA) systems. The typical standard curves for rat N-ERC/mesothelin and C-ERC/mesothelin are shown.

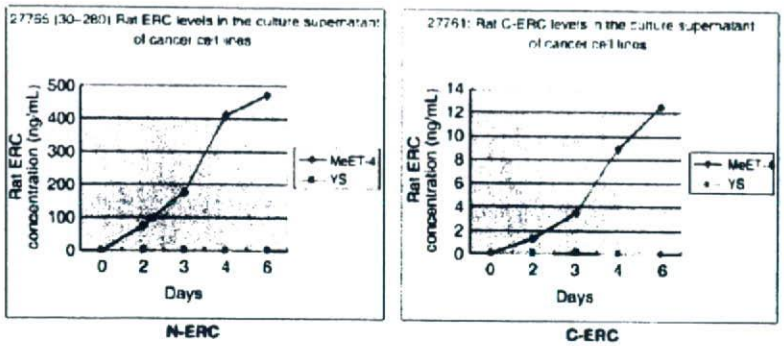

Fig. 4. Rat ERC levels in the culture supernatant of cancer cell lines. On day 0, rat mesothelioma cells (MeET-4) (◆) or Yoshida sarcoma (YS) (■) cells (5×10^4) were seeded in 24-well culture plates. At each time point, culture supernatants were taken from four wells. The concentration of rat ERC/mesothelin was determined using sandwich enzyme-linked immunosorbent assay (ELISA).

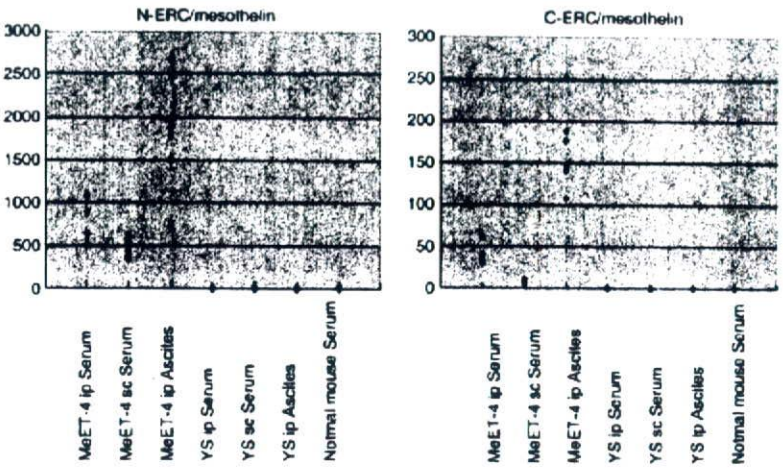

Fig. 5. Rat N- and C-ERC/mesothelin concentrations in body fluids of tumor-bearing nude mouse. The ascites with the transplantation of rat mesothelioma cells (MeET-4) or Yoshida sarcoma (YS) into the abdominal cavity (MeET-4 or YS ip ascites), serum harvested as same manner (MeET-4 or YS ip Serum), and serum harvested from mice with subcutaneous transplantations of MeET-4 or YS (MeET-4 or YS sc Serum) were measured for N- and C-ERC/mesothelin concentrations by specific enzyme-linked immunosorbent assay (ELISA) systems.

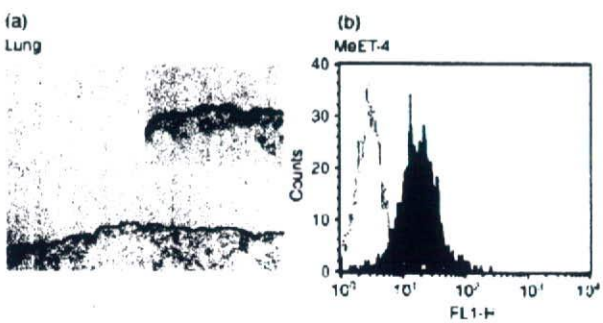

Fig. 6. The cell surface expression of rat C-ERC/mesothelin using anti-C-ERC/mesothelin antibody (306). (a) Immunohistochemical analysis in a normal rat lung. An enlarged view of a portion of stained epithelial cells was presented in upper right. (b) FACS analysis of MeET-4 mesothelioma cells.

C-ERC/mesothelin was detected on the cell surface, but N-ERC/mesothelin was not detected. This results showed that N-ERC/mesothelin fragments should be secreted into the blood or body fluid immediately after protease digestion. The mechanism of releasing C-ERC/mesothelin from the cell surface has not yet been fully elucidated. However, C-ERC/mesothelin seems to be attached to the cell surface by phosphatidylinositol. It is released when cells are treated with phosphatidylinositol-specific phospholipase C.[15]

Discussion

As mentioned earlier, there appears to be a strong relationship between ERC/mesothelin and mesothelioma caused by asbestos exposure in humans; however, the nature of the relationship or the functions of the protein have not yet been clarified at present. The rat ERC/mesothelin was detected in the blood and ascitic fluid of the nude mice transplanted with MeET-4 cells, using a specific ELISA system. This results demonstrated that the rat ERC/mesothelin is of malignant MeET-4 cell origin. In the future, we would like to clarify the relationship between the rat ERC/mesothelin found in the body fluids of MeET-4 tumor-bearing mice and mesothelioma.

The measurement range of the ELISA system for N-ERC/mesothel described by Nakaishi *et al.*[12] was between 1.25 ng/mL and 80 ng/mL. However, in this study, the novel ELISA system indicated an improved measurement range between 0.078 ng/mL and 5.0 ng/mL by using new antibodies. This improvement could achieve precise measurements in the blood and body fluids of mice.

This system should be a useful tool for elucidating the functions of ERC/mesothelin and its role in the development of mesothelioma, as well as screening and the evaluation of antimesothelioma drugs. Also, we hope these ELISA and mouse model systems will be valuable in evaluating new antimesothelioma therapies.

Acknowledgments

We thank Aki Arita, Mizuka Segawa, Shunsuke Miyai, and Kazuya Miyashita for helping in the management of this study and the critical

doi: 10.1111/j.1349-7006.2008.00731.x

reading of this manuscript. This work is supported by a Grant-in-Aid for Cancer Research and Grants-in Aid for Scientific Research from the Ministry of Education, Culture, Sports, Science, and Technology of Japan and the Ministry of Health, Labor, and Welfare of Japan.

This study was partially supported by a consignment expense for the Molecular Imaging Program on 'Research Base for PET Diagnosis' from the Ministry of Education, Culture, Sports, Science and Technology of Japan.

References

1 Hino O, Kobayashi E, Nishizawa M *et al.* Renal carcinogenesis in the Eker rat. *J Cancer Res Clin Oncol* 1995; **121**: 602–5.
2 Yamashita Y, Yokoyama M, Kobayashi E, Takai S, Hino O. Mapping and determination of the cDNA sequence of the Erc gene preferentially expressed in renal cell carcinoma in the Tsc2 gene mutant (Eker) rat model. *Biochem Biophys Res Commun* 2000; **275**: 134–40.
3 Robinson BW, Creaney J, Lake R *et al.* Mesothelin-family proteins and diagnosis of mesothelioma. *Lancet* 2003; **362**: 1612–6.
4 Scholler N, Fu N, Yang Y *et al.* Soluble member(s) of the mesothelin/megakaryocyte potentiating factor family are detectable in sera from patients with ovarian carcinoma. *Proc Natl Acad Sci* 1999; **96**: 11531–6.
5 Robinson BW, Creaney J, Lake R *et al.* Soluble mesothelin-related protein-A blood test for mesothelioma. *Lung Cancer* 2005; **49**: S109–11.
6 Hassan R, Bera T, Pastan I. Mesothelin: a new target for immunotherapy. *Clin Cancer Res* 2004; **10**: 3937–42.
7 Onda M, Willingham M, Nagata S *et al.* New monoclonal antibodies to mesothelin useful for immunohistochemistry, fluorescence-activated cell sorting, Western blotting, and ELISA. *Clin Cancer Res* 2005; **11**: 5840–6.
8 Hassan R, Remaley AT, Sampson ML *et al.* Detection and quantitation of serum mesothelin, a tumor marker for patients with mesothelioma and ovarian cancer. *Clin Cancer Res* 2006; **12**: 447–53.
9 Shiomi K, Miyamoto H, Segawa T. *et al.* A novel ELISA system for detection of a 'N-ERC/Mesothelin' in the sera of mesothelioma patients. *Cancer Sci* 2006; **97**: 928–32.
10 Maeda M, Hino O. Molecular tumor markers for asbestos-related mesothelioma: serum diagnostic markers. *Pathol Int* 2006; **56**: 649–54.
11 Hino O, Shiomi K, Maeda M. Diagnostic biomarker of asbestos-related mesothelioma: Example of translational research. *Cancer Sci* 2007; **98**: 1147–51.
12 Nakaishi M, Kajino K, Ikesue M *et al.* Establishment of the enzyme-linked immunosorbent assay system to detect the amino terminal secretory form of rat Erc/Mesothelin. *Cancer Sci* 2007; **98**: 659–64.
13 Kuwahara M, Takeda M, Takeuchi Y, Kuwahara M, Harada T, Maita K. Transforming growth factor beta production by spontaneous malignant mesothelioma cell lines derived from Fisher 344 rats. *Virchows Arch* 2001; **438**: 492–7.
14 Tsuchiya H, Tsuchiya Y, Kobayashi T, Kikuchi Y, Hino O. Isolation of genes differentially expressed between the Yoshida sarcoma and long-survival Yoshida sarcoma variants: origin of Yoshida sarcoma revisited. *Jpn J Cancer Res* 1994; **85**: 1099–104.
15 Chang K, Pastan I. Molecular cloning of mesothelin, a differentiation antigen present on mesothelium, mesotheliomas, and ovarian cancers. *Proc Natl Acad Sci* 1996; **93**: 136–40.

Pathology International 2009; **59**: 161–166 doi:10.1111/j.1440-1827.2009.02344.x

Original Article

Establishment of novel mAb to human ERC/mesothelin useful for study and diagnosis of ERC/mesothelin-expressing cancers

Kiyoshi Ishikawa,[1] Tatsuya Segawa,[1] Yoshiaki Hagiwara,[1,2] Masahiro Maeda,[1] Masaaki Abe[2] and Okio Hino[2]

[1]Immuno-bioligical Laboratories, Takasakishi, Gunma and [2]Department of Pathology and Oncology, Juntendo University School of Medicine, Hongo, Tokyo, Japan

Malignant mesothelioma is a highly aggressive tumor of the serosal cavity that arises from the mesothelial cells of the pleura, peritoneum, or pericardium. The immunohistochemical diagnosis of epithelioid mesothelioma from biopsy or surgically resected specimens has been actively pursued, using markers such as mesothelin. Several markers have indeed been helpful for confirming the diagnosis of mesothelioma and distinguishing between mesothelioma and adenocarcinoma. The authors have developed a novel mAb to human C-ERC/mesothelin, which performed well when used in western blotting, fluorescence-activated cell sorting, immunocytochemistry and immunohistochemistry, and which therefore will be useful in studying the molecular biology of mesothelin, in addition to improving the diagnosis and therapy of mesothelin-expressing cancers.

Key words: diagnosis, ERC/mesothelin, malignant mesothelioma, monoclonal antibody

Mesothelioma is an aggressive tumor arising from the serosal surface, such as the pleural and peritoneum, and it has a dismal prognosis.[1] Several recent studies have described the safe utilization of aggressive multimodality therapy and have found evidence for the effectiveness of combination chemotherapy regimens using pemetrexed and cisplatin.[2–4] The prognosis after this type of therapy, however, remains poor.

A study by Sugarbaker *et al.* reporting a 5 year survival of 40% for selected patients following trimodality therapy, demonstrated that early diagnosis is vital to improve the prognosis.[2] In light of the difficulty, however, of making an early diagnosis of mesothelioma using current diagnostic imaging techniques, the identification of tumor markers for mesothelioma is needed urgently.[5–7] While no reliable serum marker for mesothelioma has yet been found, Robinson *et al.* have recently proposed a soluble mesothelin-related protein as a candidate.[1]

Previously, we discovered the renal carcinoma gene *ERC*, which we found was expressed highly in renal cancers in the Eker rat.[8] Furthermore, we subsequently confirmed that the *ERC* gene is a homolog of the human mesothelin gene, a gene expressed strongly in normal mesothelial cells, mesothelioma, non-mucinous ovarian carcinomas and pancreatic ductal adenocarcinomas.[9,10] The human mesothelin gene codes for several proteins. Its primary product is a 71 kDa precursor protein, which is cleaved physiologically by a furin-like protease into a 40 kDa *C*-terminal fragment, C-ERC/mesothelin, which remains membrane-bound, and a 31 kDa *N*-terminal fragment, N-ERC/mesothelin, which is secreted into the blood.[11] The resultant *C*-terminal 40 kDa fragment is classified as a mesothelin, and its presence in the serum has been reported as a useful tumor marker in mesothelioma patients.[12] In contrast, the *N*-terminal 31 kDa fragment, which is a secreted protein and has been cloned as a megakaryocyte-potentiation factor, has been reported as a useful tumor marker for mesothelioma or any other cancer.[6]

In the present study we report on the establishment of a novel mAb for human C-ERC/mesothelin. This antibody should be useful in studying the molecular biology of mesothelin, and also improve the diagnosis of and therapy for mesothelin-expressing cancers.

MATERIALS AND METHODS

Human subjects

Our study for the tumor marker of mesothelioma was approved by the Institutional Review Broad of Juntendo

Correspondence: Okio Hino, MD, PhD, Department of Pathology and Oncology, Juntendo University School of Medicine, 2-1-1 Hongo, Tokyo 113-8421, Japan. Email: ohino@juntendo.ac.jp

Received 25 July 2008. Accepted for publication 3 November 2008.

University School of Medicine, its hospital, and Immuno-Biological Laboratories. Patients gave their signed informed consent.

Cell lines

The mesothelioma cell lines, NCI-H226 and MESO-4 were obtained from Dr Usami.[13] These were maintained in TIL media supplemented with 10% fetal bovine serum.

Generation of a human C-ERC/mesothelin-GST fusion protein by *Escherichia coli*

The human *C-ERC/mesothelin* cDNA was cloned from the total RNA of the human cervical carcinoma cell line HeLaS3 using polymerase chain reaction. Primers used were as follows: forward, 5′-GGAGTGGAGAAGACAGCCTGT-3′; reverse, 5′-GCCCTGTAGCCCCAGCCC-3′. cDNA for human *C-ERC/mesothelin* was inserted between the EcoRI and XhoI into pGEX-6P (GE-Healthcare Bio-sciences, Piscataway, NJ, USA). The C-ERC/mesothelin-GST fusion protein was directed into the periplasm of *E. coli*. The fusion protein was purified with Glutathione Sepharose 4B Beads (GE-Healthcare Bio-sciences). The purified proteins were quantified using Protein assay kit (Pierce, Rockford, IL, USA) and checked on sodium dodecylsulfate (SDS)-PAGE. The purity of the bacterial C-ERC/mesothelin was >95%.

Immunization and cell fusion

Female mice (6–8 weeks old; BALB/c, Charles River, Japan) were immunized four to six times weekly with human C-ERC/mesothelin-GST fusion protein (50 μg/mouse) and one boost was given with the fusion proteins i.p. before fusion. The spleen was harvested 84–90 h after the last boost and fused with X63-Ag8.653 myeloma cells.

Screening with enzyme immunoassay on human C-ERC/mesothelin-GST fusion protein

Screening for hybridomas was performed with an enzyme immunoassay (EIA). Nunc Immuno plates (Nalge Nunc International, Rochester, NY, USA) were coated with the fusion protein (50 ng/well in 0.1 mol/L carbonate buffer, pH 9.5) and incubated overnight at 4°C. Plates were then blocked with blocking buffer (PBS with 1% bovine serum albumin (BSA) and 0.05% sodium azide) overnight at 4°C and washed with a washing buffer (PBS with 0.05% Tween20). The plates were incubated with the hybridoma supernatant for 1 h at 37°C. After washing with the washing buffer, the plates were incubated with a peroxidase-conjugated goat anti-mouse IgG antibody in washing buffer. Finally, the plates were washed again with the washing buffer and hydrogen peroxide/o-phenylenediamine was added to each well. The color was allowed to develop for 15 min at room temperature and the reaction was stopped by the addition of a stop solution (1 N sulfuric acid). The plates were read at 490 nm using an automated plate reader (Molecular Device, Sunnyvale, CA, USA). The selected hybridomas were grown in a Celline flask (Integra Bioscience, Chur, Switzerland). The cell culture supernatant was affinity-purified with affinity column chromatography using Protein A column (GE-Healthcare Bio-sciences).

Epitope mapping of the anti-human C-ERC/mesothelin mouse mAb

For the determination of the epitope of the anti-human C-ERC/mesothelin mouse mAb, we produced the C-ERC/mesothelin-GST fusion protein in four different molecular sizes by cutting a human *C-ERC/mesothelin* gene into four 200 bp fragments. The fusion proteins were analyzed on western blot for epitope mapping.

Western blot

Cell lysates of the human mesothelioma cell line or C-ERC/mesothelin-GST fusion protein for epitope mapping were separated on 12.5% SDS-PAGE under reducing conditions. Proteins were transferred to a PVDF membrane (Millipore, Billerica, MA, USA). After blocking with a blocking solution (PBS with 3% non-fat dried milk, 1% BSA and 0.05% Tween20), the membrane was incubated with 1 μg/mL of each mAb overnight at 4°C, followed by a peroxidase-conjugated goat anti-mouse IgG antibody. Proteins were visualized with an ECL detection system (GE-Healthcare Bio-sciences).

Fluorescence-activated cell sorting

Cultured cells (2×10^5) were dissociated with dissociation buffer. Each sample was washed twice in fluorescence-activated cell sorter (FACS) buffer (PBS with 5% BSA, 0.1% sodium azide). An anti-human C-ERC/mesothelin mouse mAb was added to the cells and incubated for 30 min at 4°C. Cells were then washed with FACS buffer, and incubated with 2 μg/mL Alexa 488 goat anti-mouse IgG (Molecular Probe, Eugene, OR, USA) for 30 min at 4°C. Finally, cells

were washed with FACS buffer and analyzed on a FACScan system (Becton Dickinson, Franklin Lakes, NJ, USA).

Immunocytochemistry

Cultured cells or cells derived from the ascites were smeared on coverslips and air-dried for 30 min. Coverslips were fixed with cold acetone for 10 min at room temperature followed by 1% paraformaldehyde for 5 min at 4°C. Non-specific binding sites were blocked by incubating with 5% normal goat serum in PBS for 15 min at room temperature. The coverslips were incubated with the primary antibodies (2 μg/mL) for 1 h at room temperature. After washing with PBS, the coverslips were incubated with Envision+ (DakoCytomation, Kyoto, Japan), followed by detection of peroxidase with diaminobenzidine-peroxide substrate solution. The sections were counterstained with hematoxylin.

Immunohistochemistry

Formaldehyde-fixed paraffin-embedded tissue sections from patients with mesothelioma were evaluated for C-ERC/mesothelin expression. The sections were deparaffinized in xylene, followed by graded ethanol hydration into water. The sections were heated in Target Retrieval Solution, 10 mmol/L citrate buffer (pH 6.0) (DakoCytomation), for antigen retrieval. The sections were then incubated with the primary antibodies (1 μg/mL) overnight at 4°C. After washing with the washing buffer, the sections were incubated with Envision (DakoCytomation), followed by detection of peroxidase with diaminobenzidine-peroxide substrate solution. The sections were counterstained with hematoxylin.

RESULTS

Generation of recombinant human C-ERC/mesothelin-GST fusion protein with *E. coli* and establishment of new mAb for human C-ERC/mesothelin

To establish new mAb for human C-ERC/mesothelin, we generated a human C-ERC/mesothelin-GST fusion protein using *E. coli*. The fusion proteins were used for immunization and screening for the hybridoma supernatant with an EIA. Finally, eight clones were identified that reacted selectively with the fusion protein coated to plates. The specificity of the anti-human C-ERC/mesothelin mAb was determined immunohistochemically with the section from mesothelioma patients, the results of which showed that one clone from among the eight clones, 22A31, had a high affinity for human C-ERC/mesothelin. In these studies, we compared them with a commercially available mAb, 5B2 (Novocastra, Newcastle, UK), and found them to be useful in western blotting, FACS, immunocytochemistry and immunohistochemistry for human C-ERC/mesothelin.

Epitope mapping of clone 22A31, the anti-human C-ERC/mesothelin mAb

To determine the epitope of the anti-human C-ERC/mesothelin mAb, clone 22A31, we prepared four different molecular sizes of the C-ERC/mesothelin-GST fusion protein by cutting a human C-ERC/mesothelin gene into four 200 bp fragments. The fusion proteins were analyzed on western blot for epitope mapping. As a result (Fig. 1), we confirmed that the epitope 22A31 was on the *N*-terminal portion of C-ERC/mesothelin.

Western blot

The expression of human C-ERC/mesothelin in mesothelioma cell lines was analyzed on western blot (Fig. 2). This antibody detected one major product in the lysate of the

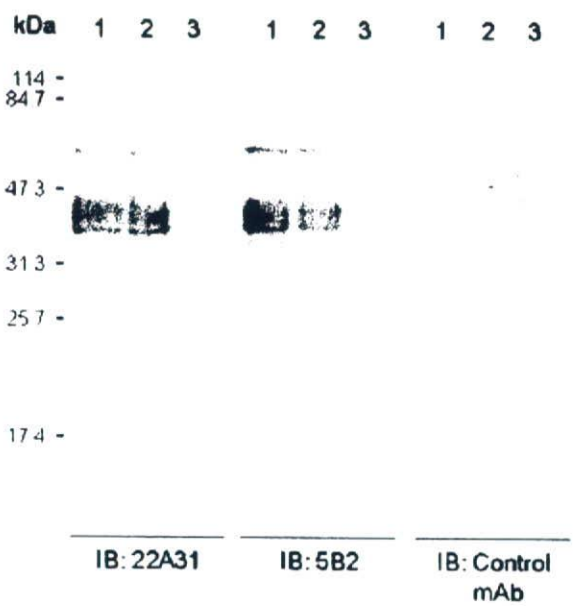

Figure 2 Western blot analysis of the clone 22A31. This antibody (1 μg/mL) detected one major product in the cell lysates of human mesothelioma cell lines, NCI-H226 (lane 1) and MESO-4 (lane 2). Control mAb did not react to the mesothelioma cell lines. Lane 3, control ERC/mesothelin-negative cell line.

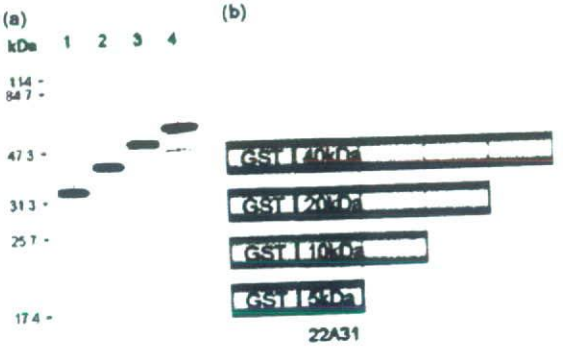

Figure 1 Epitope mapping of the clone 22A31. The epitope was on the *N*-terminal portion of C-ERC/mesothelin. (**a**) Western blot analysis for epitope mapping of (**b**) C-ERC/mesothelin-GST fusion protein in four different molecular sizes, which were produced by cutting a human C-ERC/mesothelin gene into four 200 bp fragments. The clone 22A31 reacted against every fragment. This indicates that the epitope of 22A31 was on the *N*-terminal portion of C-ERC/Mesothelin. Lane 1, GST-C-ERC/mesothelin (5 kDa); lane 2, GST-C-ERC/mesothelin (10 kDa); lane 3, GST-C-ERC/mesothelin (20 kDa); lane 4, GST-C-ERC/mesothelin (40 kDa).

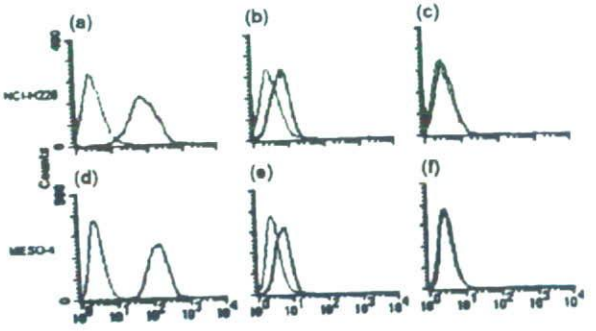

Figure 3 Fluorescence-activated cell sorting of the (**a**,**d**) clone 22A31. This antibody (2 µg/mL) bound to NCI-H226 and MESO-4. (**c**,**f**) Control mAb did not react to the mesothelioma cell lines. (**b**,**e**) 5B2.

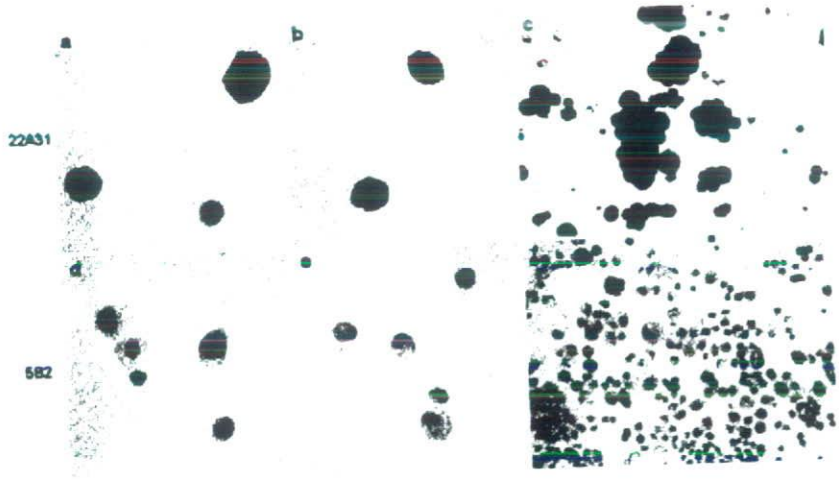

Figure 4 Immunocytochemistry of the clone 22A31. Positive staining was observed in the membranes of human mesothelioma cell lines (**a**) NCI-H226, (**b**) MESO-4 and (**c**) pleural effusion smears obtained from a mesothelioma patient. (**d**–**f**) No staining was seen with 5B2. The coverslips were incubated with the primary antibodies (2 µg/mL).

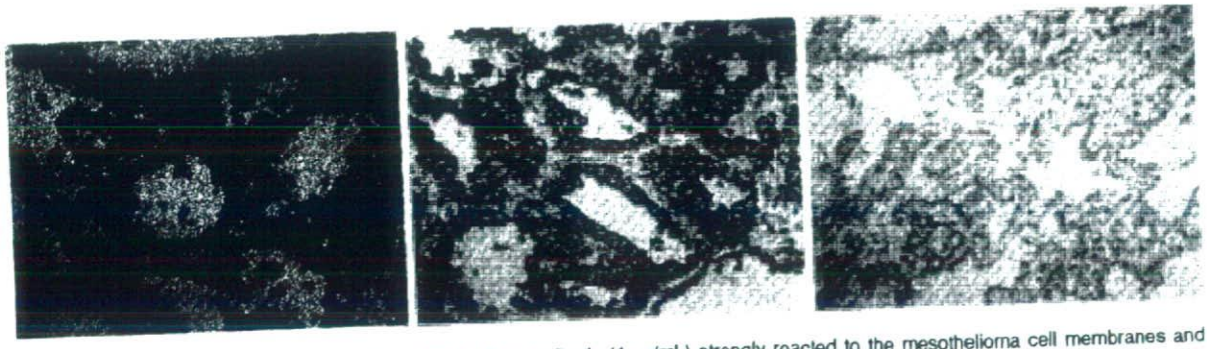

Figure 5 Immunohistochemistry of (**a**) clone 22A31. This antibody (1 µg/mL) strongly reacted to the mesothelioma cell membranes and reacted in a pattern that was comparable to (**b**) 5B2 (1:50 dilution). (**c**) Control mAb did not react to the specimens from malignant mesothelioma patients.

human mesothelioma cell lines, the molecular mass of which was approximately 40 kDa, similar to that of C-ERC/mesothelin. Control mAb did not react to mesothelioma cell lines.

Fluorescence-activated cell sorting

The clone 22A31 was tested on FACS for its ability to bind to the human mesothelioma cell lines. This antibody bound to the human mesothelioma cell lines but did not bind to the ERC/mesothelin-negative cell lines (data not shown). The data in Fig. 3 show that the clone 22A31 generated a large increase in fluorescence intensity compared with the cells incubated with the 5B2 anti-mesothelin mAb. Control mAb did not react to mesothelioma cell lines.

Immunocytochemistry

Immunocytochemical detection of C-ERC/mesothelin in smears of human mesothelioma cell lines, NCI-H226 and MESO-4, is shown in Fig. 4. Strongly positive staining was observed in membranes of these cells, which were reacted with the clone 22A31 (Fig. 4a,b). No staining was seen when the cells were incubated with the 5B2 anti-mesothelin mAb (Fig. 4d,e). The expression of C-ERC/mesothelin in pleural effusion smears obtained from malignant mesothelioma is shown in Fig. 4(c). Membranous expression was observed highly in the smears. The immunocytochemical signal was negative on smears when the 5B2 anti-mesothelin mAb was used (Fig. 4f).

Immunohistochemistry

Immunohistolocalization of ERC/mesothelin in specimens from malignant mesothelioma patients using the anti-human C-ERC/mesothelin mouse mAb is shown in Fig. 5. This antibody reacted to the mesothelioma cell membranes with a pattern that was comparable to the 5B2 anti-mesothelin mAb. This suggests that our newly established antibody could be useful in the immunohistochemical diagnosis of mesothelioma. Control mAb did not react to the specimens from malignant mesothelioma patients.

DISCUSSION

Immunohistochemical diagnosis of epithelioid mesothelioma in pleural biopsy or surgically resected specimens has been actively pursued, using markers such as podoplanin, calretinin, WT-1, cytokeratin 5, thrombomodulin, and mesothelin. Some of these markers used singly and in combination have indeed been helpful for confirming the diagnosis of mesothelioma and distinguishing between mesothelioma and adenocarcinoma, which is one of the challenging problems for the surgical pathologist. In immunohistochemistry for mesothelin, the 5B2 anti-mesothelin mAb is commonly used. In the present study, however, 5B2 had weak or negative reactivity on human mesothelioma cell lines and pleural effusion smears obtained from malignant mesothelioma patients in both FACS and immunocytochemistry. Our newly established mAb 22A31 performed well when used for western blotting, FACS, immunocytochemistry and immunohistochemistry, and could thus be useful in the detection of C-ERC/mesothelin proteins for all types of immunological assay.

The detection of ERC/mesothelin expression on immunohistochemistry and/or immunocytochemistry is important clinically to diagnose patients who are eligible for any therapeutic strategy targeting mesothelin. In addition, the detection and quantification of serum ERC/mesothelin would be helpful for the diagnosis and follow up of patients with mesothelioma, and other mesothelin-expressing cancers.

In conclusion, we have established a new mAb for human C-ERC/mesothelin that performed well in all types of immunological assay. This antibody should be useful in studying the molecular biology of mesothelin, and could also improve the diagnosis of and therapy for mesothelin-expressing cancers.

REFERENCES

1 Robinson BW, Musk AW, Lake RA. Malignant mesothelioma. *Lancet* 2005; **366**: 397–408.
2 Sugarbaker DJ, Flores RM, Jaklitsch MT *et al.* Resection margins, extrapleural nodal status, and cell type of malignant pleural mesothelioma: Results in 183 patients. *J Thorac Cardiovasc Surg* 1999; **117**: 54–63.
3 Vogelzang NJ, Rusthoven JJ, Symanowski J *et al.* Phase III study of pemetrexed in combination with cisplatin versus cisplatin alone in patients with malignant mesothelioma. *J Clin Oncol* 2003; **21**: 2636–44.
4 Sugarbaker DJ, Jaklitsch MT, Bureno R *et al.* Prevention, early detection, and management of complications after 328 consecutive extrapleural pneumonectomies. *J Thorac Cardiovasc Surg* 2004; **128**: 138–46.
5 Maeda M, Hino O. Molecular tumor markers for asbestos-related mesothelioma: Serum diagnosis markers. *Pathol Int* 2006; **56**: 649–54.
6 Shiomi K, Miyamoto H, Segawa T *et al.* A novel ELISA system for detection of a N-ERC/Mesothelin in the sera of mesothelioma patients. *Cancer Sci* 2006; **97**: 928–32.
7 Hino O, Shiomi K, Maeda M. Diagnostic biomarkers of asbestos-related mesothelioma: Example of translational research. *Cancer Sci* 2007; **98**: 1147–51.
8 Hino O, Kobayashi E, Nishizawa M *et al.* Renal carcinogenesis in the Eker rat. *J Cancer Res Clin Oncol* 1995; **121**: 602–5.

9 Yamashita Y, Yokoyama M, Kobayashi E, Takai S, Hino O. Mapping and determination of the cDNA sequence of the Erc gene preferentially expressed in renal cell carcinoma in the Tsc2 gene mutant (Eker) rat model. *Biochem Biophys Res Commun* 2000; **275**: 134–40.
10 Hino O. Multistep renal carcinogenesis in the Eker (Tsc 2 gene mutant) rat model. *Curr Mol Med* 2004; **4**: 807–11.
11 Hassan R, Bera T, Pastan I. Mesothelin: a new target for immunotherapy. *Clin Cancer Res* 2004; **10**: 3937–42.
12 Hassan R, Remaley AT, Sampson ML *et al.* Detection and quantification of serum mesothelin, a tumor marker for patients with mesothelioma and ovarian cancer. *Clin Cancer Res* 2006; **12**: 447–53.
13 Usami N, Fukui T, Kondo M *et al.* Establishment and characterization of four malignant pleural mesothelioma cell lines from Japanese patients. *Cancer Sci* 2006; **97**: 387–94.

9 Yamashita Y, Yokoyama M, Kobayashi E, Takai S, Hino O. Mapping and determination of the cDNA sequence of the Erc gene preferentially expressed in renal cell carcinoma in the Tsc2 gene mutant (Eker) rat model. *Biochem Biophys Res Commun* 2000; **275**: 134–40.
10 Hino O. Multistep renal carcinogenesis in the Eker (Tsc 2 gene mutant) rat model. *Curr Mol Med* 2004; **4**: 807–11.
11 Hassan R, Bera T, Pastan I. Mesothelin: a new target for immunotherapy. *Clin Cancer Res* 2004; **10**: 3937–42.
12 Hassan R, Remaley AT, Sampson ML *et al.* Detection and quantification of serum mesothelin, a tumor marker for patients with mesothelioma and ovarian cancer. *Clin Cancer Res* 2006; **12**: 447–53.
13 Usami N, Fukui T, Kondo M *et al.* Establishment and characterization of four malignant pleural mesothelioma cell lines from Japanese patients. *Cancer Sci* 2006; **97**: 387–94.

Available online at www.sciencedirect.com
ScienceDirect
Mutation Research 638 (2008) 48–55
Fundamental and Molecular Mechanisms of Mutagenesis
www.elsevier.com/locate/molmut
Community address: www.elsevier.com/locate/mutres

Mutagenic radioadaptation in a human lymphoblastoid cell line

Fumio Yatagai [a,*], Yukihiro Umebayashi [a], Masamitsu Honma [b], Kaoru Sugasawa [c], Yuko Takayama [a], Fumio Hanaoka [d]

[a] *Advanced Development and Support Center, The Institute of Physical and Chemical Research (RIKEN), Saitama 351-0198, Japan*
[b] *Division of Genetics and Mutagenesis, National Institute of Health Sciences, Tokyo 158-8501, Japan*
[c] *Genome Damage Response Research Unit, The Institute of Physical and Chemical Research (RIKEN), Saitama 351-0198, Japan*
[d] *Graduate Program, Frontiers in Biosciences, Osaka University, Osaka 565-0871, Japan*

Received 6 April 2007; received in revised form 15 August 2007; accepted 22 August 2007
Available online 1 September 2007

Abstract

We investigated the mutagenic radioadaptive response of human lymphoblastoid TK6 cells by pretreating them with a low dose (5 cGy) of X-rays followed by a high (2 Gy) dose 6 h later. Pretreatment reduced the 2-Gy-induced mutation frequency (MF) of the *thymidine kinase* (*TK*) gene (18.3×10^{-6}) to 62% of the original level (11.4×10^{-6}). A loss of heterozygosity (LOH) detection analysis applied to the isolated TK^- mutants revealed the mutational events as non-LOH (resulting mostly from a point mutation in the *TK* gene), hemizygous LOH (resulting from a chromosomal deletion), or homozygous LOH (resulting from homologous recombination (HR) between chromosomes). For non-LOH events, pretreatment decreased the frequency to 27% of the original level (from 7.1×10^{-6} to 1.9×10^{-6}). cDNAs prepared from the non-LOH mutants revealed that the decrease was due mainly to the repression of base substitutions. The frequency of hemizygous LOH events, however, was not significantly altered by pretreatment. Mapping analysis of chromosome 17 demonstrated that the distribution and the extent of hemizygous LOH events were also not significantly influenced by pretreatment. For homozygous LOH events, pretreatment reduced the frequency to 61% of the original level (from 5.1×10^{-6} to 3.1×10^{-6}), reflecting an enhancement in HR repair of DNA double-strand breaks. Our findings suggest that the radioadaptive response in TK6 cells follows mainly from mutations at the base-sequence level, not the chromosome level.

Keywords: Adaptive response; TK6 cells; LOH detection system

1. Introduction

An adaptive cellular response occurs when a mild stress applied before a challenging treatment with a DNA-damaging agent decreases the detrimental effects of the challenge. In radioadaptation, as it is usually defined, exposure to a low dose of ionizing radiation (IR) provides some protection against a high dose. Radioadaptation was first reported by Olivieri et al. [1], who showed that radiation delivered by labeling human lymphocytes with tritiated thymidine causes a decrease in the frequency of chromosomal aberrations induced by subsequent exposure to 15 Gy of IR. That discovery stimulated a series of studies in human lymphocytes and various mammalian cell lines (for review, see refs. [2,3]) and suggested that the adaptive response is an important defense mechanism, especially against low doses of IR. The molecular mechanisms involved, however, remain largely unknown [4–8], and cellular

* Corresponding author. Tel.: +81 48 467 9710; fax: +81 48 462 1426.
E-mail address: yatagai@postman.riken.go.jp (F. Yatagai).

0027-5107/$ – see front matter © 2007 Elsevier B.V. All rights reserved.
doi:10.1016/j.mrfmmm.2007.08.014

responses such as the bystander effect, genetic instability and hyper-radiosensitivity seem tightly related to the adaptive response in a specific low-dose region. One of the hot subjects in recent adaptive response studies is the expression of the genes involved in the mechanism [8–10]. Another is the relationship between the adaptive response and the bystander effect [11–15]. In mammalian cells, for example, bystander mutagenesis may be suppressed by an adaptive response [11].

Following the report by Olivieri et al., reduced induction of both micronuclei and sister chromatid exchanges was shown in Chinese hamster V79 cells pre-exposed to low doses of γ-rays or ^{3}H β-rays [16]. Subsequent studies reported similar radioadaptive responses, such as reduced mutation frequencies in human lymphocytes [17], mouse SR-1 cells [18] and human–hamster hybrid A_L cells [19], an altered mutation spectrum in human–hamster hybrid A_L cells [19], reduced micronucleus frequencies in human lymphocytes [5] and mouse embryo cells [20], and reduced deletions and rearrangements in human lymphoblast cells [21]. The mechanism underlying those radioadaptations may have been the induction of an efficient chromosome repair system by the priming radiation dose, and in fact, the efficiency of DNA double-strand break (DSB) repair in Chinese hamster V79 cells exposed to γ-rays is enhanced by a priming exposure of 5 cGy of γ-rays [22]. Furthermore, DSBs with either blunt or staggered ends, created by restriction enzymes, induce the adaptive response [3].

The human lymphoblastoid TK6 cell line, isolated by Skopek et al. [23], is heterozygous at the *thymidine kinase* (*TK*) locus. Honma's laboratory developed a loss of heterozygosity (LOH) detection system that can be used for molecular analysis of *TK* mutations as well as for detecting alterations at the chromosome level [24,25]. Using that methodology, we were able to detect IR effects at doses as low as 10 cGy [26–28]. Irradiation of TK6 cells with 10 cGy of X-rays clearly demonstrated radiation-specific types of LOH events or interstitial deletions in chromosome 17 [26]. We also observed more efficient induction of such events after 10 cGy irradiation with an accelerated carbon-ion (135 MeV/u) beam [27], and this was apparent in frozen cells exposed to the same carbon-ion beam [28]. These results strongly suggest that the interstitial deletions were the result of end-joining repair of IR-induced DSBs.

Because the radiation-sensitive LOH analysis system in TK6 cells is effective for detecting the fate of radiation-induced DNA double-strand breaks (DSBs), we use it here to see if the adaptive response could produce measurable changes in IR-induced genetic alterations. The results we obtained were not completely expected, but are interesting.

2. Materials and methods

2.1. Cell culture and adaptive treatment

The methodologies for the detection of *TK*-deficient mutants and the materials and methods used for cell culture and growth have been previously reported [26]. Briefly, TK6 cells were incubated in RPMI1640 medium supplemented with HAT to eliminate pre-existing TK^- deficient mutants. The cells were then resuspended in fresh normal medium, and 6 ml cell suspension was dispensed into 6-cm diameter Petri dishes. The cells were pretreated ("primed") with 2.5, 5 or 10 cGy of X-rays (250 kVp) at a rate of 10 cGy/min, and placed in a 5% CO_2 humidified incubator. The cell concentration was adjusted to 8×10^5 cells/ml at the end of the post-irradiation incubation period of 1.5, 3, 6, 9 or 12 h. The cells were then challenged with 2 Gy X-rays (250 kVp) at 1 Gy/min. Non-primed irradiated cells treated in the same manner as the primed cells served as controls.

2.2. Survival assay and TK mutation assay

To determine the surviving fraction of the challenged cells, we measured the plating efficiency (PE) immediately after irradiation using the limiting dilution method. For mutation expression, we incubated the cells with non-selecting RPMI1640 medium for about 60 h following the X-ray challenge. We measured the PE of incubated cells similarly, determining the *TK* mutation frequency. To select TK^- mutant clones, we seeded incubated cells into 96-well plates at 4×10^4 cells per well in RPMI1640 medium containing 4 μg/ml trifluorothymidine (TFT); we harvested the normally growing clones after 2 weeks and the slow growing clones after 4 weeks.

2.3. Determination of optimum irradiation conditions for mutagenic adaptation

To determine the optimum conditions for evoking the mutagenic radioadaptive-response, we tested the MF induced by 2 Gy at 0, 1.5, 3, 6, 9 and 12 h after a priming dose of 10 cGy, selected the optimum interval time, and then tested the MF induced by 2 Gy at that interval time after priming doses of 0, 2.5, 5 and 10 cGy.

2.4. LOH analysis of TK^- mutants

Fig. 1 illustrates how we classified TK^- mutants. We first determined *TK* LOH by PCR analysis of exons 4 and 7 [29]. If the PCR products of both were similar to those of the parental *TK* heterozygous cells, we classified the mutant

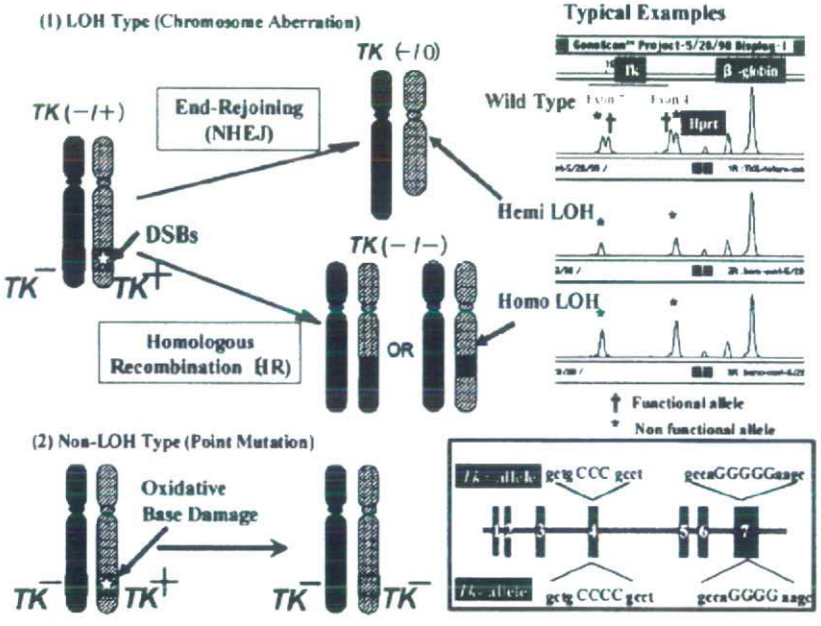

Fig. 1. LOH classifications of *TK*$^-$ mutants. The first step in the genetic analysis of selected *TK*$^-$ mutants was to judge whether there was a loss of *TK* heterozygosity (LOH). This was accomplished by PCR amplification of exons 4 and 7 regions of the *TK* locus. This step also distinguished between hemizygous LOH (loss of the functional *TK* allele) and homozygous LOH (replacement of the functional *TK* allele by a mutated *TK*$^-$ allele (see ref. [29]).

as a "non-LOH" mutant. We used the same technique to distinguish between hemizygous LOH (in which the functional *TK* allele is lost) and homozygous LOH (in which the functional *TK* allele is replaced by *TK*$^-$). To determine the extent and size of the deleted or substituted portions of the chromosome involved, we analyzed 11 microsatellite regions (D17S588, D17S1784, D17S785, D17S789, D17S802, D17S807, D17S928, D17S932, D17S1299, D17S1566 and THRA) on chromosome 17 using multiple PCR reactions as described previously [29]. The fine structure of the recovered *TK*$^-$ LOH mutations was determined by chromosome mapping analysis.

2.5. Base sequencing of non-LOH mutants

For a precise analysis of non-LOH mutants, we extracted RNA using Isogen (Nippon Gene, Japan), and obtained cDNA using a First-Strand cDNA Synthesis Kit, Amersham, USA). Following PCR amplification, the purified 807-bp fragments were sequenced by Takara Bio (Japan). The primers 5′-AGAGTACTCGGGTTCGTGAA-3′ and 5′-GCAGCATGCAGGGCAGCGTG-3′ (forward and reverse, respectively) were used for cDNA synthesis, PCR amplification and base sequencing [30]. To prevent the overestimation of mutational events, we counted identical mutations originating from a single irradiated dish as a single event.

Table 1a
TK mutation frequency (MF) at various time intervals between priming and challenging X-ray exposures (priming dose, 10 cGy; challenging dose, 2 Gy)

Time interval (h)	0	1.5	3	6	9	12
TK MF ($\times 10^{-6}$)	19.8	18.1	14.4	13.5	17.8	19.7

3. Results

3.1. Optimum conditions for mutagenic adaptation

For inducing an adaptive response to X-ray irradiation, the optimum interval between a 10-cGy priming dose and a 2-Gy challenging dose was 6 h (Table 1a), and the optimum priming dose 6 h prior to a 2-Gy challenging dose was 5 cGy (Table 1b). We therefore decided to characterize the induced *TK* mutants by repeating

Table 1b
TK mutation frequency at various priming X-ray doses (challenging dose, 2 Gy; interval between 2 exposures, 6 h)

Priming X-ray dose (cGy)	0	2.5	5	10
TK MF ($\times 10^{-6}$)	13.3	15.8	4.5	6.3

Table 2
Surviving fractions of primed and non-primed TK6 cells following challenge exposure to 2 Gy X-rays

Experiment	Surviving fraction	
	Non-primed cells	Primed cells (5 cGy)
I	0.043	0.047
II	0.047	0.070
III	0.049	0.040
Mean ± S.D.	0.046 ± 0.0031*	0.052 ± 0.016*

* $P = 0.58$; t-test.

Table 3
TK mutation frequency in primed and non-primed TK6 cells following challenge exposure to 2 Gy X-rays

Experiment	*TK* mutation frequencies ($\times 10^{-6}$)	
	Non-primed cells	Primed cells (5 cGy)
I	13.3	4.5
II	13.3	10.5
III-a	20.4	15.1
III-b	21.0	15.6
Mean ± S.D.	18.3 ± 4.3*	11.4 ± 5.1*

Experiments III-a and III-b were carried out concurrently with survival assay III, but they were independent mutation assays.
* $P = 0.020$; t-test.

our mutation experiments under those conditions (5 cGy followed 6 h later with 2 Gy).

3.2. Survival assay and TK mutation assay

Table 2 shows the surviving fraction, expressed as PE (2 Gy X-ray irradiated cells)/PE (unirradiated cells) of primed and unprimed cells immediately after the 2-Gy challenge exposure. Irradiation with the priming dose of 5 cGy did not influence the PE of unchallenged cells (data not shown). The effect of priming on survival after 2 Gy X-ray irradiation was 1.1 (0.052/0.046; $P = 0.58$, t-test). Thus, priming did not significantly affect survival after the challenge exposure.

On the other hand, priming did affect the *TK* MF induced by the challenge. Data from 4 independent experiments showed that priming reduced the MF to 62% of the unprimed MF ($P = 0.020$, t-test) (Table 3).

3.3. LOH analysis of TK^- mutants

Table 4 shows the distributions of LOH classes among the isolated TK^- mutants as determined by PCR analysis. We isolated non- and "small" LOH mutants (see Sections 3.4 & 3.5) as normal growth mutants in the first selection, except for a few cases. We isolated the remaining LOH mutants as slow growth mutants in the second selection. We estimated the pre-exposure effect from the proportion of each mutational event as follows: (i) 7.1×10^{-6} to 1.9×10^{-6} reduction in corresponding MF of non-LOH events, (ii) 6.4×10^{-6} to 6.1×10^{-6} change in corresponding MF of hemizygous LOH events and (iii) 5.1×10^{-6} to 3.1×10^{-6} reduction in corresponding MF of homozygous LOH events. Thus, the MF of a non-LOH event in primed cells was reduced to 27% of the non-primed MF. The induction of hemizygous events, on the other hand, was barely influenced by priming. As far as homozygous events go, their corresponding MF was reduced to 61% of the original level, which was similar to level of reduction in total MF (62%).

3.4. Analysis of LOH tracts on chromosome 17

Fig. 2 shows the deleted or replaced regions of chromosome 17 in each LOH mutant. Mutants reflected both type 1 and type 2 LOH events. Type 1 defines a terminal event; that is, the deleted or exchanged chromosome segment extends to the telomere marker (D17S928). Type 2 defines an interstitial deletion; the altered segment does not reach the telomere marker.

In the present study, most hemizygous LOH mutations, which are considered to be the result of DSB non-homologous end-joining (NHEJ) repair, reflected

Table 4
Distribution of mutational classes among the isolated *TK* mutants

Mutational class	Number of identified mutants (Exp. I, II, III-a, III-b) [MF $\times 10^{-6}$]	
	Non-primed cells	Primed cells (5 cGy)
Non-LOH	18 (5, 4, 6, 3) [7.1]	8 (1, 3, 2, 2) [1.9]
LOH		
Hemizygous	15 (3, 3, 7, 2) [6.0]	27 (8, 7[a], 5, 7) [6.4]
Homozygous	13 (3, 4, 3, 3) [5.1]	13 (2, 3, 5, 3) [3.1]
Total	46 (11, 11, 16, 8) [18.3]	48 (11, 13, 12, 12) [11.4]

[a] One of the seven mutants was a mixed hemizygous/homozygous type.

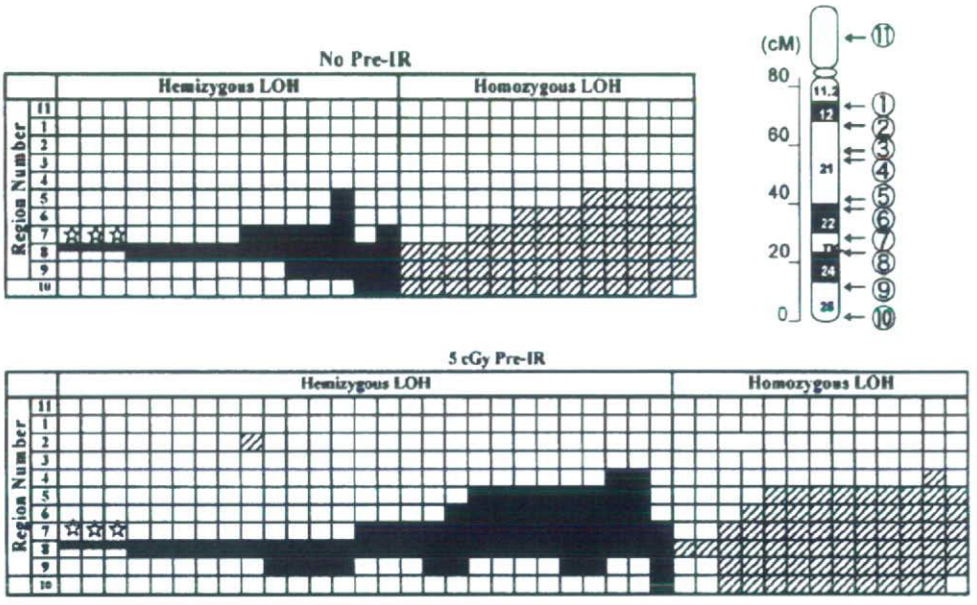

Fig. 2. Chromosome mapping of the LOH mutants. We analyzed the LOH mutants selected after a 2 Gy of challenging X-ray irradiation to determine the extent of the deleted or exchanged portions of the chromosome. The upper panel shows the profiles of 28 LOH mutants selected from non-primed cells, and the lower panel shows the profiles of 40 LOH mutants selected from cells primed with 5 cGy of X-rays. Each column represents a single LOH mutant. The rows represent regions of chromosome 17 diagrammed in the upper right insert. Shaded squares represent deleted regions and hatched squares represent exchanged regions (see text). The region numbers refer to the 11 microsatellite regions: (1) D17S588; (2) D17S1784; (3) D17S785; (4) D17S789; (5) D17S802; (6) D17S807; (7) D17S928; (8) D17S932; (9) D17S1299; (10) D17S1566; (11) THRA (see ref. [29]). The star symbol represents a "small" type 2 hemizygous event in which the deletion is restricted to *TK* locus.

type 2 events in both the non-primed (13 of 15 mutants) and primed (26 of 27 mutants) groups. Small type 2 deletions – those restricted to the *TK* locus (Fig. 2) – were infrequent in both groups (3 of 15 mutants in non-primed cells and 3 of 27 in primed cells). Similarly, the proportion of large deletion mutants (expanding to the region beyond region 8, Fig. 2) was also similar in the primed (18 of 27 mutants) and non-primed (7 of 15 mutants) groups. Homozygous LOH events, on the other hand, which are considered to be the result of homologous recombination (HR) repair of DSBs, were primarily identified as type 1 events in both primed (10 of 13) and non-primed (12 of 13) groups. Interestingly, small homozygous LOH events (where only a single region was replaced, Fig. 2) were recovered from the primed cells (2 of 13 (3 0f 14)), but not from the non-primed cells (0 of 13).

3.5. Analysis of non-LOH-mutants

We detected many types of alterations in the non-LOH mutant cDNAs (Table 5). The proportion of single base-substitutions among all the mutations identified as this class was 1/8 (13%) in the primed cells, and this value was clearly lower than 7/18 (87%) in the unprimed cells. G and C bases were targeted in base substitution mutations, except for a single case of an A to T transversion (Table 5). Most (4/5) of the double-base changes consisted of a single base deletion (causing a frameshift) and a base substitution, except for a single case of a GC to TA double transversion in a radioadapted mutant. It is difficult to estimate the effect of priming on the induction of the double-base change events from the limited number of cells involved. Similar difficulties were also found in the other mutational events in this class such as triple-base changes, multiple-base changes and exon skipping. In addition, the proportion of abnormal transcription events (both functional and non-functional *TK* alleles are equally transcribed) was also similar in the radioadapted (1/8, 13%) and the non-adapted (3/18, 17%) group, although its origin was not identified.

4. Discussion

The radioadaptation conditions used in this study (5 cGy of priming X-rays followed in 6 h by 2 Gy of challenging X-rays) were similar to those used in other studies [4,6,11,12,14,16]. The *TK* mutation frequency